

## Density Functional Study of Polycarbonate. 2. Crystalline Analogs, Cyclic Oligomers, and Their Fragments

B. Montanari, P. Ballone,<sup>†</sup> and R. O. Jones\*

*Institut für Festkörperforschung, Forschungszentrum Jülich, D-52425 Jülich, Germany*

*Received October 22, 1998; Revised Manuscript Received February 16, 1999*

**ABSTRACT:** Density functional studies have been performed for the crystalline forms of the cyclic dimer and tetramer of bisphenol A polycarbonate (BPA-PC), as well as for the isolated structural units and their fragments (including carbonic acid, benzene, phenol, monophenyl carbonate, and BPA). There are no adjustable parameters in the calculation, and the optimized structures agree well with the results of X-ray diffraction analyses where available. Calculated vibration frequencies are compared with experimental data and with earlier calculations. Ring-opening of the cyclic oligomers is an important polymerization technique, and the cyclic tetramer provides an interesting model for future calculations of reactions between polymer segments and additional molecules.

### 1. Introduction

The wide range of industrial applications of polycarbonate molecules has led to many studies of this family of polymers. Bisphenol A polycarbonate (BPA-PC) is one of the best studied, and it has become a prototype material in developing both theoretical and experimental techniques.<sup>1–3</sup> The most precise structural information available on molecules closely related to BPA-PC has come from X-ray diffraction studies. Early data on oriented chains were given by Prietzschk,<sup>4</sup> and there are two crystalline forms (referred to here as C-PC) of the diphenol carbonate of 2,2-bis(4-hydroxyphenyl)propane (BPA). The unit cells contain, respectively, two and four structural units with 59 atoms each. The first form was synthesized by Perez and Scaringe<sup>5</sup> and was designated “immobile” from the low rate of  $\pi$ -flips of the phenylene rings.<sup>6</sup> The same motion is facile in a second (“mobile”) crystalline modification of C-PC.<sup>7</sup> Finally, the cyclic dimer, trimer, and tetramer carbonates of BPA have been isolated and analyzed spectroscopically, and the structures of the crystalline forms of dimer and tetramer have been determined by X-ray diffraction.<sup>8</sup>

The present work continues a study of the applicability of the density functional (DF) method to organic molecules and molecular crystals, as well as to organic polymers. The DF formalism<sup>9</sup> is free of adjustable parameters and has obtained growing acceptance in the fields of molecules and atomic clusters. Combined with molecular dynamics (MD),<sup>10</sup> it allows us to simulate the microscopic dynamical behavior of systems and—as a form of “simulated annealing”—to avoid geometrical structures corresponding to unfavorable local minima in the energy surface. We have shown<sup>11,12</sup> that DF calculations—with the exchange-correlation energy functional proposed by Perdew, Burke, and Ernzerhof (PBE)<sup>13</sup>—provide a satisfactory description of the intermolecular interactions in crystalline polyethylene (PE) and in the mobile and immobile forms of C-PC. We have also studied torsional and rotational energy barriers in these systems, as well as the influence of the molecular packing on the motion of segments in BPA-PC. The minimum energy barrier associated with the

rotation of phenylene rings in the crystal is for the innermost such ring, and the calculated value (7.7 kcal/mol) is in satisfactory agreement with experiment.

Here we extend these calculations to the dimer and tetramer ring oligomers of BPA-PC, referred to here as PC-2 (Figure 1) and PC-4 (Figure 2), respectively. The ring topologies are more closely related to the chain structure of the polymer than are the isolated molecular units of the mobile and immobile forms. The cyclic oligomers provide insight into the structural trends as the molecules increase in length (the cyclic dimer was the first in this family to have exclusively *cis-trans* orientation about the carbonate). They are also important in their own right, not least because of the current interest in ring opening polymerization, ROP.<sup>14</sup> We also perform calculations on several fragments of the monomer [4,4'-isopropylidenediphenylbis(phenyl carbonate), DPBC], referred to below as PC-1, ranging from isomers of carbonic acid to BPA itself. The results provide further tests of the DF method and extend the database of energy surfaces that we are using to refine the parameters of a force field for modeling much larger polycarbonate systems.

Essential details of the calculations are provided in section 2. The results for the structures and vibration frequencies of molecular fragments are given in section 3, equilibrium structures of PC-molecules and solids in section 4, and the corresponding vibration frequencies in section 5. We discuss and summarize our findings in section 6, where we note two directions for future work that are of direct relevance for the polymer itself.

### 2. Method of Calculation

The method of calculation was described in detail previously.<sup>15,16</sup> The electron-ion interaction is represented by ionic pseudopotentials with the (nonlocal) form suggested by Troullier and Martins.<sup>17</sup> We adopt a plane wave basis with a kinetic energy cutoff of 35 au, and the expansion of the orbitals uses a single point ( $\mathbf{k} = 0$ ) in the Brillouin zone. Periodic boundary conditions are assumed, and we use a simple cubic cell with lattice constant 40 au<sup>18</sup> for the isolated molecules. Density functional calculations presently require an approximation to the exchange-correlation energy, and our previous calculations on organic molecular crystals<sup>11</sup> indicated that the PBE approximation, which is relatively

\* Corresponding author (e-mail: r.jones@fz-juelich.de).

<sup>†</sup> On leave from Max-Planck-Institut für Festkörperforschung, Heisenbergstr. 1, D-70569 Stuttgart, Germany.

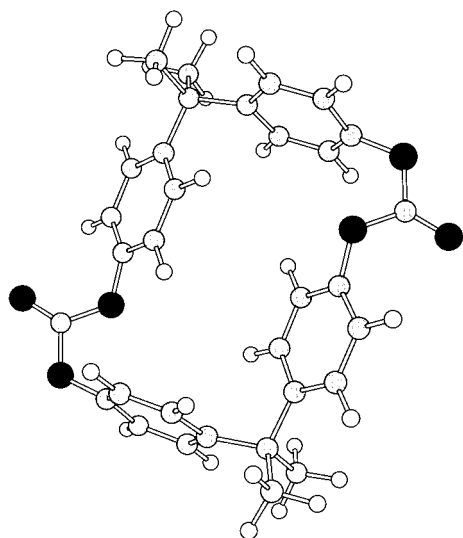


**Figure 1.** Cyclic dimer PC-2. Carbon atoms are gray, oxygen atoms black, and hydrogen atoms white.

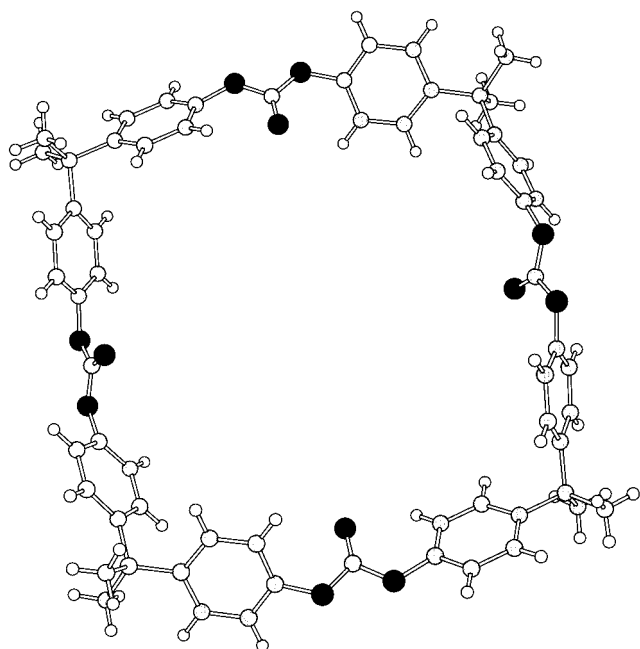


**Figure 2.** Cyclic tetramer PC-4. Carbon atoms are gray, oxygen atoms black, and hydrogen atoms white.

simple and free of empirical input, is the most reliable in this context. This functional has been used for all systems in the present study.

All structures were optimized using a combination of DF calculations with MD<sup>19</sup> and a simulated annealing strategy. The calculations were started from the atomic coordinates and unit cells determined from X-ray diffraction data of the crystalline systems<sup>8</sup> and performed without constraint (on symmetry or otherwise) until the magnitude of the *maximum* force on any atom was less than  $5 \times 10^{-4}$  au and the *average* force on the atoms was an order of magnitude less. PC-4 tends to include solvent molecules on crystallization, and the stable crystals were obtained using *m*-xylene (1,3-dimethylbenzene) as a solvent. The coordinates of *all* atoms, including those of the solvent molecules, are allowed to relax in all calculations.

The vibration frequencies and eigenvectors of the gas-phase molecules and the  $\Gamma$ -point phonons of their crystal

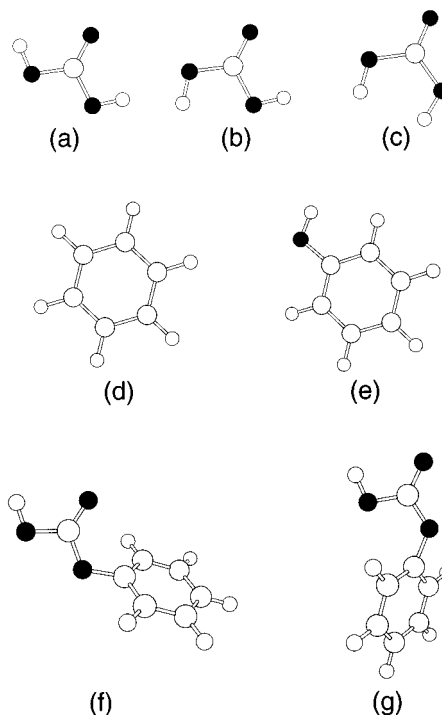


**Figure 3.** Molecular structures. (a) *trans-trans* (b) *cis-trans*, and (c) *cis-cis* isomers of carbonic acid, (d) benzene, (e) phenol, (f) *trans-trans* and (g) *trans-cis* isomers of monophenyl carbonate.

forms were calculated for the optimized geometries discussed in sections 3 and 4. The dynamical matrix **D** is evaluated by a finite difference approximation with atomic displacements  $\delta$  of the order of 0.005 Å. The computed frequencies change by at most a few wave-numbers upon increasing or decreasing  $\delta$  by a factor of 3, so that anharmonic contributions are very small.

The intensity of infrared fundamentals in absorption  $\alpha$  for a mode with frequency  $\nu_j$  is estimated by associating an electrostatic charge  $q_I$  with each atom  $I$  and evaluating

$$\alpha(\nu_j) = \frac{8\pi^3 N \nu_j}{3ch} \left| \sum_I q_I \delta \mathbf{r}_I^{(j)} \right|^2 \quad (1)$$

where  $\delta \mathbf{r}_I^{(j)}$  is the displacement of atom  $I$  for the  $j$ th vibrational eigenvector and  $N$  is the molecular density. The atomic charges are computed by a least-squares fit to the electrostatic potential around each molecule.<sup>20</sup> Equation 1 is an approximation to the quantum mechanical expression for the infrared absorption,<sup>21</sup> but should be accurate for the weakly polar, closed shell molecules considered here.

### 3. Molecular Fragments

To identify the origin of the structural details discussed for the PC oligomers, we have performed calculations of isolated molecules representing fragments of increasing size. In Figure 3 we show (a–c) isomers of carbonic acid, (d) benzene, (e) phenol, and (f, g) isomers of monophenyl carbonate, and in Figure 4, (a) 2,2-bis-(4-hydroxyphenyl)propane (BPA) and (b) DPBC. Chart 1 shows the labeling of the atoms in these systems. For each we have computed the vibrational properties, and comparison with the available experimental data allows us to assess their accuracy. Atomic coordinates, vibra-

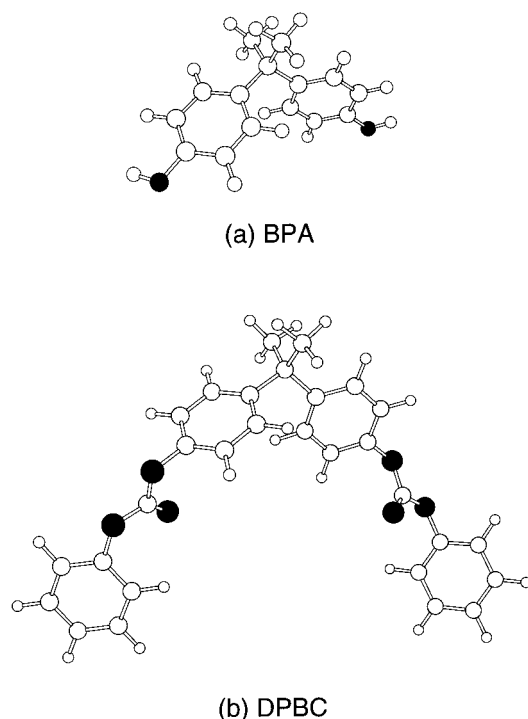
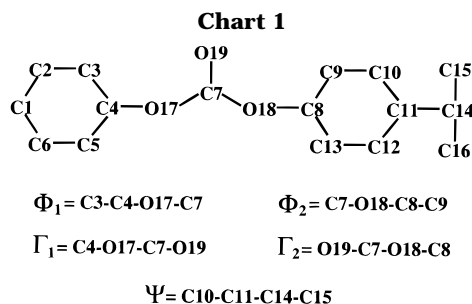


**Figure 4.** Molecular structures: (a) BPA; (b) DPBC, also denoted PC-1.



tion frequencies, and eigenvectors are available as Supporting Information.

A similar analysis could be carried out on the experimental atomic positions. However, such data are generally less extensive and homogeneous than the results of a series of well-converged calculations using the same method. Moreover, points of detail can be investigated with relative ease by performing computations on modified or artificial structures. This is seldom the case in an experimental study.

**A. Carbonic Acid.** Carbonic acid ( $\text{H}_2\text{CO}_3$ ) dissociates very rapidly into  $\text{H}_2\text{O}$  and  $\text{CO}_2$  in water at ambient temperatures, but has been synthesized recently in condensed phases at low temperatures.<sup>22,23</sup> Bonding between carbonic acid molecules will be discussed elsewhere, and we focus here on the structures of isomers of the isolated molecule, three of which represent well-defined minima in the energy surface. Structural parameters and energy differences for the *trans-trans* (Figure 3a), *cis-trans* (Figure 3b), and *cis-cis* (Figure 3c) isomers of  $\text{H}_2\text{CO}_3$  are given in Table 1, together with the results of other calculations.<sup>24,25</sup>

Energy differences in carbonic acid have proven to be very sensitive to the type of calculation performed,<sup>24,26</sup> although the structural parameters are less affected. Table 1 shows that the present calculations agree satisfactorily with the second-order Møller–Plesset

(MP2) results of ref 25. The attractive interaction between O2 and the terminal hydrogens contributes to the relative stability of the *trans-trans* conformer, while the high energy of the *cis-cis* isomer arises from the short distance between the two hydrogens (considerably less than the sum of the van der Waals radii). The dipole moments of the isomers are 0.27, 3.02, and 4.92 D for the *trans-trans*, *cis-trans* and *cis-cis* forms, respectively.

The most prominent features in the vibrational spectrum of the *trans-trans* isomer of  $\text{H}_2\text{CO}_3$  are the stretching modes of the hydroxyl groups ( $3533\text{ cm}^{-1}$ ) and of carbonyl ( $1787\text{ cm}^{-1}$ ). The out-of-plane mode with the highest frequency ( $759\text{ cm}^{-1}$ ) involves oscillations of C with respect to the plane of the oxygen atoms. All these modes are infrared active. The different conformations of the OH groups in the *cis-trans* and *cis-cis* isomers are reflected in slight shifts in the frequencies of the first two modes, while the out-of-plane motion of C is almost unaffected. In the *cis-trans* conformation the OH stretch occurs at  $3521$  and  $3511\text{ cm}^{-1}$  and the C=O stretch at  $1836\text{ cm}^{-1}$ . The corresponding modes in the *cis-cis* form are at  $3542$ ,  $3523$ , and  $1855\text{ cm}^{-1}$ . The zero point energy (square brackets in Table 1) contributes only weakly to the energy differences between the three isomers, favoring the least stable structures with the softest vibrations.

Infrared spectral studies have been performed on two low-temperature condensed phases.<sup>22,23</sup> The relationship to the vibrations of the single molecule is not immediate, however, because some frequencies in the condensed phases—in particular the OH stretch—are modified significantly by the formation of intermolecular bonds. In view of this, our results are consistent with the experimental data (the OH stretch covers the range  $1900\text{--}3200\text{ cm}^{-1}$ , the C=O stretch is at  $1702\text{ cm}^{-1}$ , and the out-of-plane  $\text{CO}_3$  bending is at  $806\text{ cm}^{-1}$ ). The results of MP2 calculations<sup>25</sup> of the vibration frequencies for the ground-state structure of  $\text{H}_2\text{CO}_3$  deviate significantly more from the experimental data.

The C=O stretch is found at  $1770\text{ cm}^{-1}$  in polycarbonate materials, while the O–H stretch at the terminal phenol of each chain is at  $3595\text{ cm}^{-1}$ .<sup>27</sup> This suggests that the carbonate group is relatively weakly perturbed in the polymers, which is quite different from the behavior in carbonic acid solids.

**B. Benzene.** Benzene is one of the best studied hydrocarbons and has served as a benchmark for both methods of calculation and measurements on other systems.<sup>28</sup> In Table 2, we compare the measured geometry<sup>29</sup> with the present results (PBE functional) and those of DF calculations with the LD approximation<sup>30</sup> and a commonly used nonlocal modification (BLYP).<sup>30,31</sup> Our structures agree well with experiment and with the earlier calculations.

The simplicity and high symmetry of benzene allow a detailed comparison of computed vibrational frequencies with experimental data. It is important to note that the peaks in measured vibrational spectra are affected by anharmonic effects and do not correspond exactly to the harmonic frequencies. In benzene, for example, the observed peaks can differ by up to  $120\text{ cm}^{-1}$  from the corresponding harmonic frequencies.<sup>28</sup> As shown in Table 3, our computations describe the (corrected) harmonic frequencies in benzene well. Apart from the lowest energy modes, for which the finite difference scheme is less reliable, the calculated and experimental

**Table 1. Bond Lengths (Å) and Angles (deg) and Differences in Total and Zero Point Energy ( $\Delta E$ ,  $\Delta E_{\text{ZP}}$ , kcal/mol) in Carbonic Acid Isomers<sup>a</sup>**

struct param	<i>trans-trans</i>	<i>cis-trans</i>	<i>cis-cis</i>
C7-O19	1.217 (1.188, 1.218)	1.208 (1.180, 1.208)	1.202 (1.172, 1.201)
C7-O17	1.353 (1.315, 1.345)	1.371 (1.316, 1.344)	1.371 (1.333, 1.366)
C7-O18	1.353 (1.315, 1.345)	1.351 (1.333, 1.364)	1.371 (1.333, 1.366)
O17-H17	0.984 (0.951, 0.969)	0.985 (0.950, 0.969)	0.982 (0.947, 0.966)
O18-H18	0.984 (0.951, 0.969)	0.985 (0.952, 0.969)	0.982 (0.947, 0.966)
O19-C7-O17	125.8 (125.1, 125.9)	125.4 (124.4, 125.4)	121.6 (122.1, 122.4)
O19-C7-O18	125.8 (125.1, 125.9)	124.1 (124.6, 124.3)	121.6 (122.1, 122.4)
H17-O17-C7	105.0 (107.9, 106.1)	105.6 (108.3, 106.7)	112.5 (115.0, 111.9)
H18-O18-C7	105.0 (107.9, 106.1)	108.4 (110.8, 109.1)	112.5 (115.0, 111.9)
H17...O19	2.320 (2.291, ...)	2.336 (2.299, ...)	3.062 (2.996, ...)
H18...O19	2.320 (2.291, ...)	3.036 (2.975, ...)	3.062 (2.996, ...)
H18...O17	3.022 (2.966, ...)	2.170 (2.993, ...)	2.385 (3.340, ...)
H17...O18	3.022 (2.966, ...)	3.057 (2.159, ...)	2.385 (3.340, ...)
H17...H18	3.720 (3.670, ...)	3.134 (3.096, ...)	2.024 (2.027, ...)
$\Delta E$	0.00	1.50 (2.44, 1.86)	10.0 (12.29, 11.76)
$\Delta E_{\text{ZP}}$	0.00	-0.49 (-0.46, -0.38)	-1.78, (-1.90, ...)

<sup>a</sup> H atoms take the labels of the adjacent C atom. Values in parentheses are HF/6-31G\*<sup>24</sup> and MP-2 results<sup>25</sup> (no nonbonding differences), respectively.

**Table 2. Bond Lengths (Å) and Angles (deg) in the Benzene Molecule**

atoms	PBE (this work)	exptl <sup>29</sup>	LDA <sup>30</sup>	BLYP <sup>30</sup>
C-C	1.397	1.399	1.385	1.400
C-H	1.093	1.101	1.092	1.086

**Table 3. Vibration Frequencies of Benzene, C<sub>6</sub>H<sub>6</sub> (cm<sup>-1</sup>)<sup>a</sup>**

$\nu$	present work	obsd	est harmonic
1	3127.5	3073.9	3191
2 (2)	3120.0	3064.4	3181
3 (2)	3105.6	3057	3174
4	3095.6	3056.7	3174
5 (2)	1587.8	1601.0	1606
6 (2)	1459.5	1484.0	1494
7	1404.5	1350	1367
8	1322.9	1309.4	1309.4
9 (2)	1157.9	1177.8	1177.8
10	1141.8	1149.7	1149.7
11	1033.0	1038.3	1038.3
12	1029.1	1010	1010
13	997.5	993.1	994.3
14 (2)	987.7	990	990
15 (2)	971.6	967	967
16 (2)	897.1	847.1	847.1
17	800.6	674.0	674.0
18	731.4	707.1	707
19 (2)	601.6	608.1	607.8
20 (2)	494.0	398	398

<sup>a</sup> The experimental results are from ref 28, and degeneracies are given in parentheses.

values differ by at most 3%. This level of agreement is consistent with our earlier work on organic molecules and shows that modern DF schemes lead to vibration frequencies that are within a few percent of experiment. The accuracy of averaged vibrational properties, e.g., the zero point energy (ZPE,  $E_{\text{ZP}}$ ), should be even higher. In benzene the calculated ZPE differs from the experimental value by only ~0.1%.

The comparison, however, is less satisfactory if we compare the frequencies of modes with a given symmetry (Table 4),<sup>32</sup> where some mismatches occur in pairs and correspond to the interchange in the role of eigenvectors with the same symmetry. We have observed this in previous studies of highly symmetric molecules and attribute it to subtle differences between the theoretical and experimental potential energy surfaces.

**C. Phenol.** Table 5 compares the experimental structural parameters<sup>33</sup> of phenol (Figure 3e) with the present results and with those of earlier DF calculations<sup>34</sup> using the BLYP and B3LYP functionals.<sup>31</sup> Costa Cabral et al.<sup>34</sup> also carried out Hartree-Fock and MP2

**Table 4. Harmonic Frequencies  $\omega_i$  (cm<sup>-1</sup>) for Vibrational Modes of Benzene of Specific Symmetry<sup>a</sup>**

$\omega$	symmetry	present work	exptl <sup>28</sup>
$\omega_1$	A <sub>1g</sub>	3127.5	3191
$\omega_2$	A <sub>1g</sub>	987.7	994.4
$\omega_3$	A <sub>2g</sub>	1322.9	1367
$\omega_4$	A <sub>2u</sub>	800.6	674.0
$\omega_5$	B <sub>1u</sub>	3119.7	3174
$\omega_6$	B <sub>1u</sub>	993.7	1010
$\omega_7$	B <sub>2g</sub>	997.5	990
$\omega_8$	B <sub>2g</sub>	731.4	707
$\omega_9$	B <sub>2u</sub>	1157.9	1309.4
$\omega_{10}$	B <sub>2u</sub>	1404.5	1149.7
$\omega_{15}$	E <sub>2g</sub>	3015.6	3174

<sup>a</sup> We use the mode numbering of Herzberg.<sup>32</sup>

**Table 5. Bond Lengths (Å) and Angles (deg) in the Phenol Molecule<sup>a</sup>**

atoms	PBE (this work)	exptl <sup>33</sup>	BLYP/6-31G* <sup>34</sup>	B3LYP/6-311G** <sup>34</sup>
C1-C2	1.396	1.395	1.405	1.392
C2-C3	1.396	1.394	1.406	1.393
C3-C4	1.400	1.391	1.410	1.396
C4-C5	1.400	1.391	1.410	1.397
C5-C6	1.394	1.392	1.403	1.390
C6-C1	1.398	1.395	1.408	1.395
C1-H1	1.092	1.080	1.093	1.083
C2-H2	1.093	1.084	1.094	1.084
C3-H3	1.095	1.086	1.097	1.087
C4-O17	1.379	1.375	1.384	1.367
O17-H17	0.982	0.957	0.981	0.962
C5-H5	1.092	1.081	1.093	1.083
C6-H6	1.093	1.084	1.094	1.084
C1-C2-C3	120.5	120.5	120.5	120.5
C2-C3-C4	119.8	119.4	119.7	119.8
C3-C4-C5	120.1	120.8	120.1	119.9
C4-C5-C6	119.5	119.2	119.5	119.6
C5-C6-C1	120.8	120.8	120.8	120.8
C6-C1-C2	119.3	119.2	119.3	119.3
C1-C2-H2	120.2	119.8	120.2	120.2
H3-C3-C4	119.9	120.0	119.9	119.9
C3-C4-O17	122.6	117.0	117.2	117.4
C4-O17-H17	108.1	108.7	108.0	109.1
C4-C5-H5	119.0	120.0	118.9	118.8
C5-C6-H6	119.2	119.5	119.2	119.3

<sup>a</sup> H atoms take the label of the adjacent C atom.

calculations on phenol and showed that the DF calculations gave a good description of its structure. Our results show that this is also true for the PBE functional.

The ground state structure is almost exactly planar, and the C3-C4-O17 angle, adjacent to the OH group, is larger than the C5-C4-O17 angle. We attribute this to an intrinsic asymmetry of O17, which has the hydrogen atom on one side and two lone pairs on the



**Table 6. Harmonic Frequencies  $\omega_i$  (cm<sup>-1</sup>, in Order of Increasing Energy) and Zero Point Energy  $E_{\text{ZP}}$  (kcal/mol) for Phenol**

mode	exptl <sup>35</sup>	DF (BLYP) <sup>34</sup>	present work
$\omega_1$	244	226	295
$\omega_2$	309	388	400
$\omega_3$	404	394	419
$\omega_4$	409	406	488
$\omega_5$	503	499	522
$\omega_6$	527	521	570
$\omega_7$	619	617	611
$\omega_8$	687	674	725
$\omega_9$	752	732	804
$\omega_{10}$	817	787	808
$\omega_{11}$	823	805	846
$\omega_{12}$	881	844	891
$\omega_{13}$	973	905	954
$\omega_{14}$	995	935	974
$\omega_{15}$	1000	985	984
$\omega_{16}$	1026	1020	1014
$\omega_{17}$	1070	1073	1062
$\omega_{18}$	1177	1162	1143
$\omega_{19}$	1150	1171	1147
$\omega_{20}$	1169	1183	1155
$\omega_{21}$	1262	1254	1234
$\omega_{22}$	1277	1335	1311
$\omega_{23}$	1343	1355	1410
$\omega_{24}$	1472	1476	1451
$\omega_{25}$	1502	1502	1472
$\omega_{26}$	1604	1593	1588
$\omega_{27}$	1610	1605	1596
$\omega_{28}$	3027	3078	3086
$\omega_{29}$	3049	3099	3106
$\omega_{30}$	3063	3107	3114
$\omega_{31}$	3070	3123	3128
$\omega_{32}$	3087	3131	3133
$\omega_{33}$	3656	3587	3541
$E_{\text{ZP}}$ (kcal/mol)	128.4		127.3

other, and to the short distance between OH and the closest hydrogen (H3) in the ring. The present calculations gave a dipole moment of 1.26 D, in good agreement with the measured value (1.224 D).<sup>33</sup>

In Table 6, we compare our calculated harmonic frequencies of phenol with the results of a previous DF study<sup>34</sup> and with experimental data.<sup>35</sup> In this case, the experimental spectrum has not been reanalyzed to estimate the harmonic frequencies, and the comparison is less direct than in benzene. Nevertheless, the agreement of computed and measured frequencies is satisfactory, with deviations of at most ~3%. The OH stretch frequency (3541 cm<sup>-1</sup>) is almost the same as in carbonic acid, and the computed ZPE differs from the experimental one by less than 1%.

**D. Monophenyl Carbonate.** Isomers of this molecule have been studied previously using Hartree-Fock and DF methods,<sup>24,36</sup> and results for the *trans-trans* (Figure 3f) and *cis-trans* (Figure 3g) forms are compared with ours in Table 7. There is good overall agreement between the results, particularly between the two DF sets.

The most interesting structural feature in this molecule is the asymmetry in the O17-C4 (1.413 Å) and O17-C7 (1.359 Å) bond lengths.<sup>37</sup> As noted in ref 24 and discussed for the C-PC molecular unit,<sup>12</sup> this asymmetry reflects the enhanced  $\pi$ -bonding contribution to the O17-C7 bond. The CO<sub>3</sub> unit is close to planar as a result, and this feature should persist in the oligomers discussed below.

As in phenol, the C3-C4-O17 and C5-C4-O17 angles deviate from the ideal value (120°) in both the *trans-trans* and *cis-trans* isomers. Moreover, the O17

**Table 7. Structure and Energy Parameters (Bond Lengths in Å, Angles in deg, Energy Differences  $E$  and  $E_{\text{ZP}}$  in kcal/mol) in Monophenyl Carbonate<sup>a</sup>**

struct param	<i>trans-trans</i>	<i>cis-trans</i>
C7-O19	1.214 (1.185, 1.208)	1.213 (1.182)
C7-O17	1.359 (1.319, 1.344)	1.356 (1.321)
C7-O18	1.359 (1.318, 1.345)	1.362 (1.323)
O17-C4	1.413 (1.385, 1.399)	1.414 (1.385)
O18-H18	0.985 (0.951, 0.968)	0.986 (0.952)
O19-C7-O17	128.0 (126.9, 127.5)	121.3 (122.5)
O19-C7-O18	125.4 (124.7, 125.4)	124.9 (124.3)
C4-O17-C7	118.7 (119.8, 118.6)	125.2 (122.7)
H18-O18-C7	104.5 (107.5, 106.0)	104.1 (107.4)
C5-C4-O17	122.6 (120.9, 121.6)	123.6 (119.1)
C3-C4-O17	115.5 (117.3, 116.5)	114.7 (119.1)
C5-C4-O17-C7	47.9 (63.5, 59.2)	49.2 (91.9)
H3...O19	2.562 (2.838)	4.030 (4.163)
$\Delta E$	0.0	3.36 (2.47)
$\Delta E_{\text{ZP}}$		[+0.2]

<sup>a</sup> H atoms take the label of the adjacent C atom. The results in brackets are from HF/6-31G\* and DF calculations (*trans-trans* only).<sup>24</sup>

atom is slightly (0.1 Å) out of the plane of the aromatic carbon ring. This effect is probably due to the short-range repulsion between H3 and the carbonyl oxygen, which also causes the C3-C4-O17-C7 torsional angle ( $\Phi_1$ ) to deviate significantly from planar ( $\Phi_1 = 48^\circ$  in both isomers).

We know of no previous calculations or measurements of the vibrational frequencies of monophenyl carbonate. The OH stretch is the same in the *trans-trans* and *cis-trans* forms (the difference is less than 10 cm<sup>-1</sup>) and remarkably close to the frequency observed in the smallest fragment, H<sub>2</sub>CO<sub>3</sub>. The modes localized on the carbonyl group are more sensitive to the local bonding environment: the stretching frequency is 1772 cm<sup>-1</sup> in the *trans-trans* and 1800 cm<sup>-1</sup> in the *cis-trans* isomer, and the corresponding values for the out-of-plane motion of C7 are 751 and 743 cm<sup>-1</sup>. The highest C-H stretching frequency (3153 cm<sup>-1</sup>) involves the C3-H3 bond, with other C-H stretching modes being at least 20 cm<sup>-1</sup> lower in energy. This feature is found in all molecules with a short O19-H3 distance and appears to be a consequence of the interaction between these two atoms. The C-O single bond stretch occurs at 1179 cm<sup>-1</sup>, significantly lower than in polycarbonate materials (1220 cm<sup>-1</sup>).<sup>27</sup>

**E. 2,2-Bis(4-hydroxyphenyl)propane, BPA.** The last fragment we will discuss is BPA (Figure 4a), which is the vertex joining successive carbonate units in BPA-PC chains. Selected structural parameters and vibrational frequencies are reported in Table 8. The ground-state structure has *C*<sub>2</sub> symmetry, with the methyl groups in the eclipsed geometry. The orientation of the two phenylene rings is determined by the short-range repulsion between the phenyl and methyl hydrogen atoms (minimum H-H distance of 2.19 Å), and the two phenyl groups are nearly perpendicular. The lowest frequency for rotation of the phenylene rings is 200 cm<sup>-1</sup>, and the OH stretch frequency is very close to that of phenol. The C-H stretching modes of methyl and phenyl form two narrow bands intermediate between the OH frequency and the frequency of the modes involving carbon.

We know of no other computations for this molecule, although static DF calculations have been performed

**Table 8. Selected Structural Parameters and Vibrational Frequencies in 2,2-Bis(4-hydroxyphenyl)propane (BPA)**

atoms	dist (Å)	atoms	dist (Å)
O18–H18	0.981	C10–C11	1.399
O18–C8	1.380	C11–C14	1.539
C8–C9	1.396	C14–C15	1.545
C9–C10	1.398		
atoms	angle (deg)	atoms	angle (deg)
H18–O18–C8	108.0	C12–C11–C14	119.6
O18–C8–C9	123.0	C11–C14–C15	112.2
O18–C8–C13	117.5	C15–C14–C16	107.6
C10–C11–C14	123.1		
H18–O18–C8–C9	0.9	C10–C11–C14–C11'	131.6
C10–C11–C14–C15	12.1		
mode	frequency (cm <sup>-1</sup> )	mode	frequency (cm <sup>-1</sup> )
OH str	3549, 3557	OC str	1242
CH (phenyl) str	3086–3135	out-of-plane OH	474, 484
CH (methyl) str	2970–3063		

**Table 9. Bond Lengths (Å) and Angles (deg) in the Molecular Units of PC-1, PC-2, and PC-4<sup>a</sup>**

atoms	PC-1	PC-4	PC-2
C3–C4	1.394	1.397, 1.389	1.389, 1.394
C4–O17	1.410	1.411, 1.412	1.410, 1.419
O17–C7	1.364	1.363, 1.366	1.367, 1.373
C7–O19	1.210	1.211, 1.210	1.206
C10–C11	1.400	1.406, 1.400	1.402, 1.406
C11–C14	1.540	1.540, 1.542	1.547, 1.541
C14–C16	1.544	1.545, 1.544	1.542, 1.542
H3–O19	2.494	2.662, 2.337	2.954
H9–O19	3.000	2.717, 2.558	4.533
C3–C4–O17	123.2	122.7, 125.3	123.5
C5–C4–O17	115.1	116.2, 114.0	115.0
C4–O17–C7	119.2	118.7, 121.5	121.3
O17–C7–O19	128.0	127.6, 128.1	127.5
O18–C7–O19	126.9	127.4, 127.2	122.8
O17–C7–O18	105.1	105.0, 104.7	109.6
C9–C8–O18	121.2	122.3, 123.1	119.4
C13–C8–O18	117.5	116.6, 115.9	119.8
C3–C4–O17–C7 (Φ <sub>1</sub> )	44.8	52.7, 31.4	70.3
C9–C8–O18–C7 (Φ <sub>2</sub> )	69.3	55.4, 46.8	73.4
C4–O17–C7–O19	0.0	2.0, 3.8	21.0
C8–O18–C7–O19	0.5	3.0, 4.3	194.9
C10–C11–C14–C15 (Ψ)	8.4	12.8, 12.0	5.8

<sup>a</sup> Hydrogen atoms take the number of the adjacent C atom.

on the closely related 2,2-diphenylpropane.<sup>24</sup> The structural parameters reported for this molecule are similar to those found in the present study.

#### 4. Structures

In this section we discuss the structures of crystalline forms of polycarbonate and the molecular components. The isolated unit in the C–PC forms<sup>12</sup> (4,4'-isopropylidenediphenylbis(phenyl carbonate, DPBC, Figure 4b) is referred to below as PC-1. The structures of the dimer (PC-2, Figure 1) and tetramer (PC-4, Figure 2) ring oligomers have been optimized, as well as those of crystalline PC-2 and PC-4. The starting structures in the crystalline forms were the experimental atomic positions.<sup>8</sup>

**A. Isolated Molecules: PC-1, PC-2, and PC-4.** Structural parameters for PC-1, PC-2, and PC-4 are given in Table 9. The bond lengths and angles at the isopropylidene vertex and in the carbon rings are almost identical with those in the corresponding fragments,

although there are small differences near the junction of the carbonate and phenylene groups. Ring closing generally induces strain and an increase in the total energy, and both should be greater in PC-2 than in PC-4. PC-2 is less flexible than the others and adopts—uniquely in this family—the *cis-trans* conformation for its carbonyl group (the others have the *trans-trans* conformation). The total energy (without zero-point energy corrections, see section 5A) of PC-4 is 27 kcal/mol lower than that of two PC-2 units.

Several details are of interest. The first, also noted in ref 12, is that the O17–C4 bond is longer and weaker than the O17–C7 bond, which has a stronger  $\pi$ -component. This is evident in the force constants associated with the  $\Phi$  and  $\Gamma$  torsional angles, where rotations around O17–C4 require significantly less energy than those around O17–C7. Second, the angles C3–C4–O17 and C5–C4–O17 deviate by  $\sim 5^\circ$  from the ideal value ( $120^\circ$ ) in PC-1 and PC-4, but are close to  $120^\circ$  in PC-2.<sup>38</sup> This asymmetry is significant when the C–C–O–R torsional angle  $\Phi$  is close to planar and vanishes when  $\Phi \sim 90^\circ$ , independent of the residue R. The C3–C4–C5 angle is close to  $120^\circ$  in all cases. This feature, discussed above for phenol and monophenyl carbonate, arises from the asymmetry in the electron distribution around the O atom and the relatively strong interaction between H3 and R when separated by less than  $\sim 3$  Å. The same interaction causes a small ( $\sim 0.1$  Å) deviation of the O17 atom from the C3–C4–C5 plane in monophenyl carbonate, PC-1, and some of the carbonate groups in PC-2 and PC-4.

The torsional angles  $\Phi$ ,  $\Psi$  and  $\Gamma$ , shown in Table 9 for the isolated PC-1, PC-2, and PC-4 molecules, are associated with weak restoring forces and are the most susceptible to changes in stress and symmetry. There is no stress at the carbonyl group in the PC-1 unit:  $\Gamma_1$  and  $\Gamma_2$  are close to planar, and the softer  $\Phi$  angles are determined by the O19–H3 and O19–H9 distances. The torsional angles in PC-4 are similar to those in PC-1. The PC-2 molecule is the most strained of the three; the  $\Gamma$  angles depart significantly from the planar configuration, with larger deviations in the  $\Phi$  and  $\Psi$  angles.

The bond angles adjacent to the carbonyl group are also sensitive to the molecular size. The angles O19–C7–O17 and O19–C7–O18, which are equivalent in PC-1 and PC-4, differ in PC-2 ( $127.5$  and  $122.8^\circ$ ), because of the asymmetric *cis-trans* conformation of this molecule. Stress in PC-2 is also reflected in the angle O17–C7–O18 ( $110^\circ$ ), which is  $5^\circ$  larger than in PC-1 and PC-4.

**B. Crystalline PC-2 and PC-4.** The structures of the crystalline forms of the cyclic dimer (Figure 5, monoclinic) and tetramer (Figure 6, monoclinic) have been optimized. In line with our earlier experience with the mobile and immobile forms of C–PC,<sup>12</sup> all computations have been performed with the experimental unit cells. The relaxed atomic positions agree very well with the experimental data. The rms deviations for the coordinates of all atoms are 0.097 and 0.134 Å for PC-2 and PC-4, respectively, and the corresponding values for the non-hydrogen atoms are 0.018 and 0.041 Å. These deviations arise from slight rotations of the functional groups, and the computed and experimental values for interatomic distances and bond angles agree very well.

Compared with the wide range of torsional angles in the different oligomers, and some variation in the carbonate geometries, the structural changes on forming

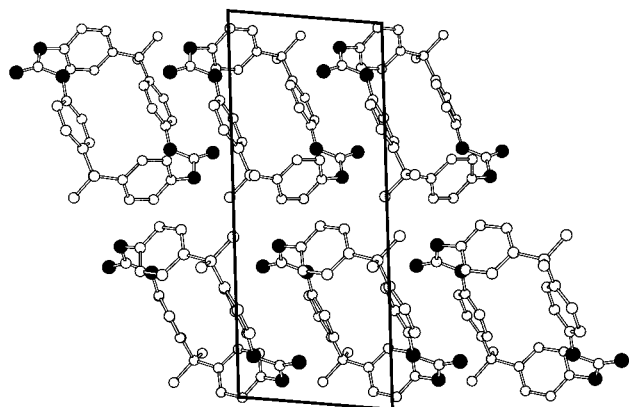


**Figure 5.** Projection of the structure of crystalline PC-2 onto the *ac*-plane. Carbon atoms are gray and oxygen atoms black. Hydrogen atoms are not shown.

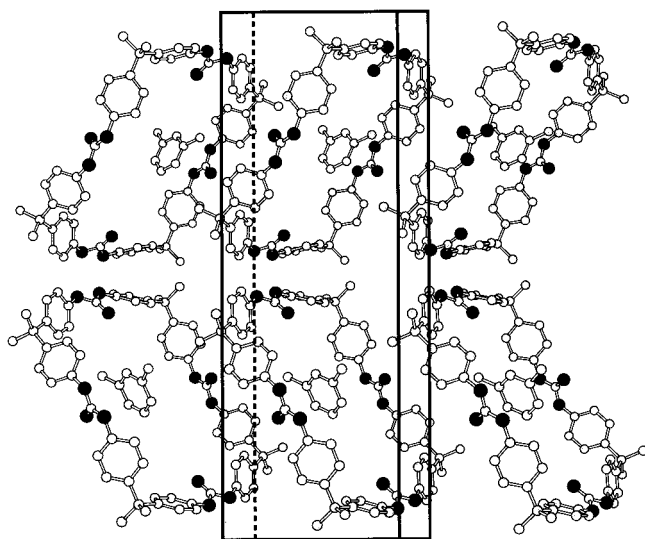


**Figure 6.** Projection of the structure of crystalline PC-4 onto the *bc*-plane. Carbon atoms are gray and oxygen atoms black. Hydrogen atoms are not shown.

crystalline PC-2 and PC-4 are small and affect primarily the soft  $\Phi$  torsional angles (see Table 9). The changes are less pronounced in PC-2 than in PC-4, reflecting the fact that the strain present in the former make it less susceptible to the intermolecular perturbations in the condensed phase.

Only the opposite edges in PC-4 are equivalent, and there are two types of conformation about the carbonate (see Figure 2). The first has a nearly symmetric position of the phenylene rings with respect to the plane of the carbonate ( $\Phi_1 \approx \Phi_2$ ), while  $\Phi_1$  and  $\Phi_2$  differ by  $\sim 15^\circ$  in the other (see Table 9).

## 5. Vibration Frequencies

The vibrational frequencies of the PC-1, PC-2, and PC-4 molecules have been computed as described in section 2 and are provided as Supporting Information. The calculated harmonic frequencies differ by up to  $\sim 3\%$  from the experimental frequencies, the absolute error in the highest energy modes being  $\sim 50 \text{ cm}^{-1}$ . However, most errors introduced by the PBE approximation should be systematic and lead to frequency differences that are much more reliable than the frequencies themselves.

This is confirmed by the comparison of the frequency for three representative modes (C–H and C–C stretch;

**Table 10.** Comparison of Computed (First Line) and Measured (Second Line, in Parentheses) Frequencies ( $\text{cm}^{-1}$ ) for (1) C–H and (2) C–C Stretch, and (3) C out-of-Plane Modes in Benzene and Phenol

mode	benzene	phenol	$\Delta$
1	3127.5	3133.6	6.1
	(3073.9)	(3087)	16.1
2	1587.8	1596.1	8.3
	(1601.0)	(1610)	9
3	997.5	974.6	−22.9
	(993.1)	(973)	−20.1

C out-of-plane) in benzene and phenol (Table 10). Anharmonic corrections have not been published for phenol, and we compare the computed harmonic frequencies with the *observed* ones for both molecules. The *shift* in the individual frequencies from benzene to phenol is reproduced very well, and frequency differences on the order of  $10 \text{ cm}^{-1}$  can be identified reliably. Moreover, properties related to low moments of the vibrational density of states, such as the zero point energy, should be relatively insensitive to the numerical uncertainties and given accurately. The comparison of the computed and measured ZPE for benzene shows that they agree to within 1%. For these reasons, we focus on the frequency *shifts* induced by changes in the molecular structure.

We note that only a few vibrational eigenstates of organic molecules of this size have a well-defined character, e.g., stretching or bending of specific atoms or bonds, while most involve the coupled motion of different groups and bond types. The exceptions are the C–H stretch modes, which are well separated at high frequencies, and the C=O stretch, which gives rise to a narrow, isolated band at  $\sim 1750 \text{ cm}^{-1}$ .

**A. Isolated Molecules: PC-1, PC-2, and PC-4.** We now discuss the trends in the vibration frequencies of the isolated PC-1, PC-2 and PC-4 molecules on the basis of the vibration spectra of the molecular fragments discussed in section 3. Calculations of PC-1 were described previously,<sup>12</sup> but the new results on the fragments allow them to be analyzed further. The calculated spectra of PC-1, PC-2, and PC-4 are similar, and we show that of PC-2 in Figure 7. We note here that PC-1 and PC-4 have the *trans–trans* conformation around the carbonate group, while PC-2 has the *cis–trans*.

The highest frequencies in PC-1 ( $3113\text{--}3166 \text{ cm}^{-1}$ ) arise from (aromatic C)–H stretching modes and are higher and have a broader spread than in the isolated benzene ring ( $3097\text{--}3128 \text{ cm}^{-1}$ ). The highest frequency is associated with the hydrogen closest to O19. A similar shift in the spectrum of monophenyl carbonate (Figure 3f) indicates that it comes from the steric repulsion between the H atom and the carbonyl oxygen atom.

The stretching modes of the C–H bonds in the two methyl groups of PC-1 occur in a range ( $2972\text{--}3079 \text{ cm}^{-1}$ ) that is slightly higher but not significantly broader than that in the isopropylidene fragment ( $2969\text{--}3063 \text{ cm}^{-1}$ ), suggesting that they are determined by the local interactions at the molecular vertex. The carbonyl C=O stretch ( $1775 \text{ cm}^{-1}$  in PC-1) is also slightly higher than in the isolated  $\text{H}_2\text{CO}_3$  molecule. A broad band ( $1470\text{--}1600 \text{ cm}^{-1}$ ) corresponds to the stretching modes of the carbon backbone. Carbon stretch is mixed with C–H bending at lower frequencies, and the C–(tetrahedral O) stretch occurs at  $1210 \text{ cm}^{-1}$ . There are modes between  $1010$  and  $1200 \text{ cm}^{-1}$  that preserve the planarity



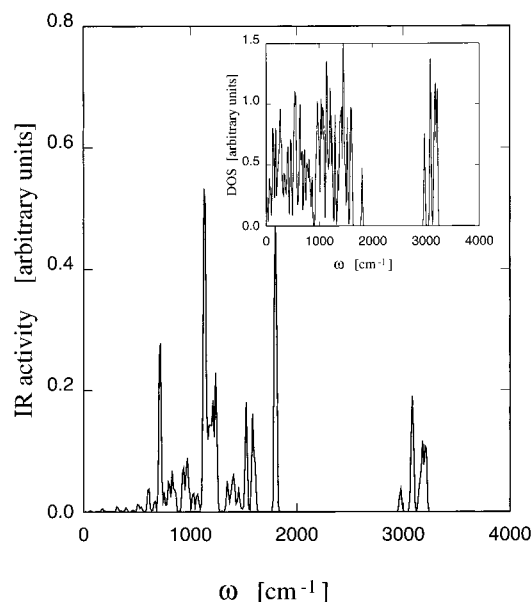


**Figure 7.** The infrared active vibrational spectrum of PC-2. The inset shows the total vibrational density of states. Each mode is represented by a Gaussian distribution of width  $12\text{ cm}^{-1}$ .

of the phenylene rings and of the carbonate groups, and out-of-plane vibrations of these groups occur between 400 and  $1000\text{ cm}^{-1}$ .

The strain in PC-2 leads to higher vibration frequencies than those in PC-1 and PC-4. The (aromatic C)–H stretch band ( $3146\text{--}3216\text{ cm}^{-1}$ ) is  $\sim 50\text{ cm}^{-1}$  higher than that in PC-1, and a similar shift is observed for the out-of-plane modes of the phenylene rings. A smaller shift ( $\sim 25\text{ cm}^{-1}$ ) occurs for some in-plane bending modes of the aromatic C atoms and for those of the H–C–H angles in the methyl groups. Stretching modes of the aromatic C–C bonds and of the C–H bonds in the methyl groups are very similar in PC-1 and PC-2.

The frequencies of the modes located on the carbonyl group are affected most by the change in conformation from PC-1 to PC-2, with both positive and negative frequency shifts. The in-plane bending modes of the carbonate group involving the O–C–O and O=C–O shift by  $\sim 50\text{ cm}^{-1}$ , and the C=O stretching mode in PC-2 is  $26\text{ cm}^{-1}$  higher than that in PC-1. The out-of-plane bending modes of the carbonate are very similar in PC-1 and PC-2.

It is interesting to compare PC-4 and PC-2, which have the same relative composition of phenylene, carbonyl, and isopropylidene groups. The PC-4 structure is less strained than PC-2, and its frequencies are generally close to those of PC-1. The ZPE of two PC-2 molecules is  $16.6\text{ kcal/mol}$  higher than that of one PC-4, and it contributes significantly to the enhanced stability of the latter. The highest frequency band [(aromatic C)–H stretching modes] lies between  $3113$  and  $3185\text{ cm}^{-1}$  in PC-4, compared with the ranges in PC-1 ( $3113\text{--}3166\text{ cm}^{-1}$ ) and PC-2 ( $3146\text{--}3216\text{ cm}^{-1}$ ). Similar trends are evident in the vibrations involving the C=O bond and in the isopropylidene bending modes.

The differences in the structures around the carbonate group lead to interesting features. In PC-1 and PC-4, for example, the highest frequency in the spectrum is associated with the (aromatic C)–H stretching modes for the H atoms closest to the carbonyl O19. On the other hand, the highest frequency mode in PC-2 involves

the H between C13 and O18. The in-plane bending modes involving O19 are softer in PC-2 ( $718\text{ cm}^{-1}$ ) than in either PC-1 ( $844\text{ cm}^{-1}$ ) or PC-4 ( $846\text{ cm}^{-1}$ ), reflecting the larger distance between this atom and H3.

It is interesting to compare the calculated frequencies with those measured by infrared absorption of PC-2 and PC-4 in the solvent  $\text{CDCl}_3$ .<sup>8</sup> The calculated carbonyl vibration band frequencies in PC-2 ( $1196\text{--}1209\text{ cm}^{-1}$ ) are lower than the measured values ( $1233\text{ cm}^{-1}$ ), and this is also true in PC-4 (calculated  $1216\text{--}1233\text{ cm}^{-1}$ ; measured  $1230\text{--}1249\text{ cm}^{-1}$ ). The calculated carbonyl absorption band in PC-2 ( $1799\text{--}1801\text{ cm}^{-1}$ ) is higher than that in PC-4 ( $1779\text{--}1782\text{ cm}^{-1}$ ), and this is also found in the measurements (PC-2,  $1780.5\text{ cm}^{-1}$ ; PC-4,  $1770.4\text{ cm}^{-1}$ ).

**B. Immobile Form of C–PC.** We have reported calculations of the vibration spectrum of the isolated molecular unit of C–PC (DPBC, PC-1) previously,<sup>12</sup> and we now present results for the immobile form of C–PC, the structure of which was optimized in ref 12.

The vibrational bands are naturally broader in immobile C–PC than in PC-1, and the spectral center of mass is slightly higher. The ZPE of C–PC—for the unit cell containing two PC-1 units—is  $7.8\text{ kcal/mol}$  higher than that in two PC-1 molecules. The most pronounced effect on the vibrations is in the (aromatic C)–H stretching modes: in the crystal they occur between  $3110$  and  $3192\text{ cm}^{-1}$ ; i.e., this band is broader and  $\sim 30\text{ cm}^{-1}$  higher than that in the isolated DPBC molecule. Analysis of the eigenvectors suggests that the shift is due to repulsion between H atoms in phenylene groups of different molecules.

**C. Crystalline PC-2 and PC-4.** We now study the effect of the molecular packing in the crystal phases of the ring oligomers. The differences between the isolated molecules and the crystal phase are largest in PC-2, with (aromatic C)–H stretching modes lying between  $3130$  and  $3168\text{ cm}^{-1}$ , i.e.,  $\sim 50\text{ cm}^{-1}$  lower than in the gas phase. A frequency lowering of  $\sim 30\text{ cm}^{-1}$  is also observed for the C=O stretch. We note that the condensed phase of the dimer has the highest density ( $1.28\text{ g/cm}^3$ ) of the crystalline polycarbonates considered here. The ZPE (per unit cell) is  $9\text{ kcal/mol}$  higher in the solid than in the isolated molecules.

## 6. Discussion and Concluding Remarks

We have performed density functional calculations to optimize the structures of the crystalline modifications of the dimer and tetramer ring oligomers of bisphenol A polycarbonate (BPA–PC), as well as for their isolated structural units and several molecular fragments. All atomic positions in the unit cell are optimized in all cases. If the unit cell is constrained to have the experimental dimensions, DF calculations with the PBE form of the exchange-correlation energy functional reproduce the measured structures very well. The harmonic vibration frequencies are calculated and compared with experimental data where available, and determination of the corresponding eigenvectors allows us to determine the nature of the vibration for the individual eigenvalues.

The results are encouraging for several reasons. The first is that calculations can indeed be performed on systems of this size and complexity using a method that is free of adjustable parameters. Unlike methods based on parametrized force fields, DF calculations can be used to describe systems where chemical bonds are



formed or broken, and we anticipate that applications to model polymer systems will provide valuable information. Moreover, we find that much structural information is transferable from the molecular fragments to the larger systems, which enables us to isolate the effects of *submolecular* interactions. A comparison of the results for the isolated molecules and for the crystalline forms of PC-1, PC-2, and PC-4 has provided information about *intermolecular* interactions.

The molecules considered here can be viewed as segments of the chains found in the BPA-PC polymer. The most stable conformation around the carbonate group is generally *trans-trans*, although the energies of the *cis-trans* conformations is only slightly higher. Strain in the ring dimer (PC-2) is sufficient to favor the latter. Both conformations are present in amorphous BPA-PC, and infrared spectroscopy of the solid carbonate suggests that the less favored conformation is stabilized by interchain forces.<sup>39</sup>

The present work has focused on crystalline forms of BPA-PC, the forms for which the most detailed structural information is available. The comparison between calculated and measured structures shows that the DF calculations provide a reliable description. We are extending this work in two distinct directions that make direct contact with the polymer itself: (a) The present calculations provide detailed information about the energy surfaces of all the above systems, not just in the neighborhood of the energy minima. This information can be used to refine the parameters of force field models, which remain indispensable for performing simulations on much larger systems over longer periods of time. Such simulations are in progress. (b) Ring-opening polymerization of the cyclic oligomers has been used as a means of preparing long BPA-PC chains. The mechanism of ring-breaking by an additional molecule is important in this context, and it is being studied by DF calculations. Furthermore, the interaction between the cyclic tetramer and such a molecule provides a model for chain-molecule interactions in general. We are performing DF calculations for the reactions between the cyclic tetramer and three additional molecules: phenol, lithium phenoxide, and sodium phenoxide.

**Acknowledgment.** The calculations were performed on the Cray T3E-600/512 and T3E-900/256 computers in the Forschungszentrum Jülich with grants of CPU time from the Forschungszentrum and the John von Neumann-Institut für Computing (NIC). The work is supported by the MaTech Program (03N8008E0) of the Bundesminister für Bildung, Wissenschaft, Forschung und Technologie, Bonn. We thank O. Hahn and other participants in this program for helpful discussions, and D. J. Brunelle and M. F. Garbaskas for providing atomic coordinates for crystalline PC-2 and PC-4 and information about their measurements.

**Supporting Information Available:** Tables of atomic coordinates, vibration frequencies, and eigenvectors. This material is available free of charge via the Internet at <http://pubs.acs.org>.

## References and Notes

- Hutnik, M.; Argon, A. S.; Suter, U. W. *Macromolecules* **1991**, *24*, 5970.
- Tomaselli, M.; Robyr, P.; Meier, B. H.; Grob-Pisano, C.; Ernst, R. R.; Suter, U. W. *Macromolecules* **1996**, *29*, 1663.
- See, for example, Goetz, J. M.; Wu, J.; Yee, A. F.; Schaefer, J. *Macromolecules* **1998**, *31*, 3016, and references therein.
- Prietzsch, A. *Kolloid Z.* **1957**, *156*, 8.
- Perez, S.; Scaringe, R. P. *Macromolecules* **1987**, *20*, 68.
- Henrichs, P. M.; Luss, H. R. *Macromolecules* **1988**, *21*, 860.
- Henrichs, P. M.; Luss, R. H.; Scaringe, R. P. *Macromolecules* **1989**, *22*, 2731.
- Brunelle, D. J.; Garbaskas, M. F.; *Macromolecules* **1993**, *26*, 2724.
- See, for example, Jones, R. O.; Gunnarsson, O. *Rev. Mod. Phys.* **1989**, *61*, 689; *Density Functional Theory*; Gross, E. K. U., Dreizler, R. M., Eds.; NATO ASI Series, Series B, Physics, No. 337; Plenum: New York, 1995.
- Car, R.; Parrinello, M. *Phys. Rev. Lett.* **1985**, *55*, 2471.
- Montanari, B.; Ballone, P.; Jones, R. O. *J. Chem. Phys.* **1998**, *108*, 6947, and references therein.
- Montanari, B.; Ballone, P.; Jones, R. O. *Macromolecules* **1998**, *31*, 7784.
- Perdew, J. P.; Burke, K.; Ernzerhof, M. *Phys. Rev. Lett.* **1996**, *77*, 3865.
- Brunelle, D. J. In *Ring-Opening Polymerization: Mechanisms, Catalysis, Structure, Utility*; Brunelle, D. J., Ed.; Hanser: München, Germany, 1993; pp 1, 309.
- Borrmann, A.; Montanari, B.; Jones, R. O. *J. Chem. Phys.* **1997**, *106*, 8545.
- Montanari, B.; Jones, R. O. *Chem. Phys. Lett.* **1997**, *272*, 347.
- Troullier, N.; Martins, J. M. *Phys. Rev. B* **1991**, *43*, 1993.
- The molecule is oriented to maximize the smallest distance between periodic replicas. Computations with a cubic unit cell of 40 au show that the calculated structures are independent of the spatial periodicity in the computation.
- Hutter, J., et al. CPMD program version 3.0, Max-Planck-Institut für Festkörperforschung und IBM Research 1990–1998.
- See, for instance, Hawkins et al. (Hawkins, G. D.; Cramer, C. J.; Truhlar, D. G. *J. Chim. Phys. (Paris)* **1997**, *94*, 1448–1481) for a discussion of electrostatic charges derived from quantum chemistry computations.
- Herzberg, G. *Infrared and Raman Spectra*; Van Nostrand Reinhold: New York, 1945; p 259 ff.
- Moore, M. H.; Khanna, R. K. *Spectrochim. Acta* **1991**, *47A*, 255.
- Hage, W.; Liedl, K. R.; Hallbrucker, A.; Mayer, E. *Science* **1998**, *279*, 1332.
- Sun, H.; Mumby, S. J.; Maple, J. R.; Hagler, A. T. *J. Phys. Chem.* **1995**, *99*, 5873.
- Wight, C. A.; Boldyrev, A. I. *J. Phys. Chem.* **1995**, *99*, 12125.
- Liedl, K. R.; Sekušak, S.; Mayer, E. *J. Am. Chem. Soc.* **1997**, *119*, 3782.
- Brunelle, D. J. In *Kirk-Othmer Encyclopedia of Chemical Technology*, 4th ed.; Kroschwitz, J. I., Howe-Grant, M., Eds.; Wiley-Interscience: New York, 1996; Vol. 19, pp 584–608.
- Goodman, L.; Ozkabak, A. G.; Thakur, S. N. *J. Phys. Chem.* **1991**, *95*, 9044.
- CRC Handbook of Chemistry and Physics*, 76th ed.; Lide, D. R., Ed.; CRC Press: Boca Raton, FL, 1995; p 9–25.
- Meijer, E. J.; Sprik, M. *J. Chem. Phys.* **1996**, *105*, 8684. The nonlocal calculations used the BLYP functional.<sup>31</sup>
- BLYP: exchange functional of Becke, A. D. *Phys. Rev. A* **1988**, *38*, 3098; correlation functional of Lee, C.; Yang, W.; Parr, R. G. *Phys. Rev. B* **1988**, *37*, 785 (LYP). B3LYP: exchange approximation of Becke, A. D. *J. Chem. Phys.* **1993**, *98*, 1372; correlation functional of LYP.
- See ref 21, p 363.
- Larsen, N. W. *J. Mol. Struct.* **1979**, *51*, 175.
- Costa Cabral, B. J.; Bakker Fonseca, R. G.; Martinho Simões, J. A. *Chem. Phys. Lett.* **1996**, *258*, 436.
- Bist, H. D.; Brant, J. C. D.; Williams, D. R. *J. Mol. Spectrosc.* **1967**, *24*, 402.
- The DF calculations used an energy functional incorporating a component of the exact exchange energy. See: Becke, A. D. *J. Chem. Phys.*, **1993**, *98*, 5648. The basis set was a double- $\zeta$  Gaussian basis with polarization functions.
- The distances refer to the *trans-trans* isomer. The *cis-trans* isomer displays a very similar asymmetry, as can be seen in Table 7.
- In ref 12 we attributed this asymmetry to the O19–H distance, but it is also observed in the phenol molecule.
- Schmidt, P.; Dybal, J.; Turska, E.; Kulczycki, A. *Polymer* **1991**, *32*, 1862.

MA981649F